Gray et al. BMC Evolutionary Biology 2011, 11:131
http://www.biomedcentral.com/1471-2148/11/131

BMC Evolutionary Biology

RESEARCH ARTICLE Open Access

The mode and tempo of hepatitis C virus evolution within and among hosts

Rebecca R Gray[1,2†], Joe Parker[3†], Philippe Lemey[4], Marco Salemi[1,2], Aris Katzourakis[5] and Oliver G Pybus[5*]

Abstract

Background: Hepatitis C virus (HCV) is a rapidly-evolving RNA virus that establishes chronic infections in humans. Despite the virus' public health importance and a wealth of sequence data, basic aspects of HCV molecular evolution remain poorly understood. Here we investigate three sets of whole HCV genomes in order to directly compare the evolution of whole HCV genomes at different biological levels: within- and among-hosts. We use a powerful Bayesian inference framework that incorporates both among-lineage rate heterogeneity and phylogenetic uncertainty into estimates of evolutionary parameters.

Results: Most of the HCV genome evolves at ~0.001 substitutions/site/year, a rate typical of RNA viruses. The antigenically-important *E1/E2* genome region evolves particularly quickly, with correspondingly high rates of positive selection, as inferred using two related measures. Crucially, in this region an exceptionally higher rate was observed for within-host evolution compared to among-host evolution. Conversely, higher rates of evolution were seen among-hosts for functionally relevant parts of the *NS5A* gene. There was also evidence for slightly higher evolutionary rate for HCV subtype 1a compared to subtype 1b.

Conclusions: Using new statistical methods and comparable whole genome datasets we have quantified, for the first time, the variation in HCV evolutionary dynamics at different scales of organisation. This confirms that differences in molecular evolution between biological scales are not restricted to HIV and may represent a common feature of chronic RNA viral infection. We conclude that the elevated rate observed in the *E1/E2* region during within-host evolution more likely results from the reversion of host-specific adaptations (resulting in slower long-term among-host evolution) than from the preferential transmission of slowly-evolving lineages.

Keywords: hepatitis C substitution rate, virus evolution, Bayesian phylogenetics, molecular clock, relaxed clock, adaptation

Background

Rapidly-evolving RNA viruses that establish chronic infections, such as the human immunodeficiency virus (HIV) and the hepatitis C virus (HCV), appear to exhibit qualitatively different evolutionary dynamics when their genetic diversity is studied at different organisational scales [1,2]. Within-host evolutionary dynamics can be observed by comparing sequences that represent different virions sampled from a single infected individual over several years, whereas among-host evolution is revealed by collating sequences that each represent a different infected host. The most significant distinction between these two levels is that the evolution of among-host sequences is shaped by numerous genetic bottlenecks arising from transmission events, whereas that of within-host sequences is not.

The hepatitis C virus (HCV) (family *Flaviviridae*, genus *Hepacivirus*) infects more than 180 million people worldwide and is a leading global cause of liver disease and liver cancer [3,4]. Understanding the evolution of HCV has considerable medical relevance. For example, viral diversity is known to play a key role in determining both the outcome of long-term chronic infection and the likelihood of success of anti-viral drug therapy [5-10]. However, despite the wealth of HCV sequence data and the relevance of HCV genetic diversity to public health, many aspects of HCV molecular evolution are

* Correspondence: oliver.pybus@zoo.ox.ac.uk
† Contributed equally
[5]Department of Zoology, Oxford University, South Parks Road, Oxford, OX1 3PS, UK
Full list of author information is available at the end of the article

poorly understood, particularly in comparison to HIV, despite HCV having a higher overall global prevalence that HIV. One of the most fundamental aspects of HCV evolution is its genomic rate of molecular evolution. Previous estimates of HCV evolutionary rates have employed a number of different estimation methods, genome regions and scales of analysis, hindering direct comparisons, and few have systematically considered the variation in evolutionary rate along the whole HCV genome and its causes [11]. The HCV genome encodes a single polyprotein ~3000 amino acids in length, comprising three structural (*Core*, *E1* and *E2*) and seven non-structural genes (*p7*, *NS2, NS3*, *NS4a, NS4b, NS5a* and *NS5b*) [12]. The *E2* envelope glycoprotein contains 'hyper-variable regions' (HVRs) that are targeted by the human humoral immune response [13]. An additional limitation of previous studies is that they have typically assumed that evolutionary rates are constant among lineages and through time (known as the 'strict' or 'single rate' molecular clock hypothesis). Although statistical tests of this hypothesis for HCV are not always significant (e.g. [14,15]), such failures to reject the strict clock are most likely a reflection of small sample sizes, because larger HCV data sets indicate significant among-lineage rate variability [11,16]. Furthermore, previous studies have typically evaluated HCV rates using a single estimated phylogeny, thus ignoring an important source of statistical error (although [11] approximated this error through bootstrapping procedures). Many previous studies used non-phylogenetic methods (such as the relative-rates test) to estimate the HCV evolutionary rate, which are now known to be less efficient and potentially more biased than phylogenetic approaches [17].

Previous analyses of HCV molecular evolution also have been restricted to a single evolutionary scale. It has been demonstrated that the evolutionary dynamics of HIV differ substantially among levels of organisation [2,18]. For example, HIV-1 within-host evolutionary rates are higher [1] and more variable [19] than those among-hosts. Although the biological causes of these differences are as yet unknown, possible explanations include preferential transmission of slowly-evolving lineages, a decreasing within-host evolutionary rate through time, or viral reversion to variants of higher fitness upon transmission to a new host [1]. Crucially, it is not known whether these scale-dependent differences are peculiar to HIV-1 or whether other chronic viral infections, such those caused by HCV, exhibit similar behaviour. Detailed investigation of multi-level evolution in viral populations - for which much data are available - may help to build a more general understanding of this complex evolutionary phenomenon.

Here, for the first time, we quantify and compare the within- and among-host molecular evolution of whole HCV genomes. We avoid the methodological limitations outlined above by analysing whole genome sequences and employing a 'relaxed molecular clock' approach that explicitly models and estimates the level of rate variation among lineages [20]. This approach is implemented in a Bayesian inference framework [21] that incorporates phylogenetic uncertainty into estimates of evolutionary parameters. In addition to employing powerful methods of analysis, we study the entire HCV genome using a partition approach, thereby revealing how scale-dependent evolution affects different viral genome regions in different ways.

Methods

Datasets

We compiled three datasets, one representing only evolution within infected hosts, the other two representing evolution at the 'epidemiological' or among-host level. To maximise compatibility and statistical power, we sought data sets comprising sequences from the same subtype sampled over at least 20 years, and which contain complete or near-complete viral genomes.

Our within-host data set is based on HCV subtype 1b genomes obtained from 15 women who were all infected by a contaminated blood product (anti-D immunoglobulin) that had been generated from a single HCV-infected blood donation ([22]; coloured red in all figures). This data set comprises full-length genomic HCV sequences from 15 patients, sampled at two time-points, plus an additional sequence sampled in 1977 from the HCV-infected blood donation (n = 31; sampling dates range from 1977 to 2000; [23]. Since the contaminated blood product contained little viral diversity [24], all recipients were infected with very similar viral sequences; hence this data set represents - perhaps uniquely - 15 independent within-host evolutionary histories, yet contains no secondary transmission events. Among-lineage rate variation in these sequences therefore reflects in equal part variation in evolutionary rate among infected hosts and among different lineages within a host. Accession numbers and isolate sampling dates of all sequences used in this study are listed in Additional file 1, Table S1.

We obtained two data sets representing evolution at the among-host level. We collected all available HCV genotype 1 whole genome sequences from the Broad Institute database http://www.broadinstitute.org/annotation/viral/HCV. These genomes were split into two data sets, comprising 334 subtype 1a and 149 subtype 1b genomes, respectively. In all figures the subtype 1a data set is coloured green and the subtype 1b data set coloured blue. Sequences were primarily collected in the USA (n = 377) as well as from Switzerland (n = 88) and Germany (n = 18). To aid computational efficiency, the subtype 1a and 1b datasets were reduced in size,

resulting in two final alignments comprising 63 subtype 1a and 54 subtype 1b sequences. Retained sequences were chosen such that the original temporal range of the initial dataset (1989-2008) was maintained, by randomly excluding sequences from over-represented years. Both among-host data sets represent HCV evolution across several decades of epidemic transmission, hence each branch in their phylogenies will represent a number of transmission events.

Model selection procedure

To select the best-fitting evolutionary model for Bayesian MCMC inference, we performed an initial series of model selection analyses using BEAST v1.5.4. MCMC output was inspected for convergence by visual inspection of the chain and by calculation of effective sample size statistics, as implemented in Tracer v1.5 http://tree.bio.ed.ac.uk. Where necessary, MCMC operators were optimised by trial and error to improve chain mixing. Various different substitution, coalescent and molecular clock models were compared by calculating Bayes Factors (BF), which is the difference in log marginal likelihoods between two model combinations [25,26]. We calculated approximate marginal likelihoods for each model via importance sampling using the harmonic mean of the sampled likelihoods (with the posterior as the importance distribution; see [27]). Evidence against the null model (i.e. the model with lower marginal likelihood) is indicated by 2ln(BF) >3 (positive evidence) and >10 (strong evidence).

In all datasets, nucleotide sites were assigned to two partitions: (i) 1^{st} & 2^{nd} codon positions and (ii) 3^{rd} codon positions. Our preliminary analyses indicated that a good fit to the data was obtained by ascribing a separate HKY nucleotide substitution model and a separate gamma among-site rate heterogeneity model to each of the two codon partitions (equivalent to the model described in [28]). This substitution model was sufficiently computationally-efficient to permit MCMC convergence (data not shown) and was therefore used throughout the remainder of the study. For the within-host data set, phylogenetic priors were used to represent known epidemiological information about the transmission chain: specifically, all sequences from the infected patients (i.e. all except the single sequence from the infected blood donation) were constrained to be a monophyletic group, and a prior normal distribution was imposed on the date of the common ancestor of this group (mean = 25 years before present and variance = 1 year).

Both strict and relaxed molecular clock models were tested for each of the three datasets using the Bayes Factor test as described above. The uncorrelated lognormal relaxed molecular clock model (UCLN) was used, which provides an estimate of the 'coefficient of variation' statistic, representing the scaled variance in evolutionary rate among lineages (see [20] for details). This statistic is usefully interpreted as indicating the degree to which molecular evolution is 'clock-like'. A posterior distribution for the coefficient of variation that does not include zero indicates that the relaxed clock model provides a better fit to the data than the strict clock. Having chosen the optimal molecular clock model for each data set, we tested three different coalescent models: (i) constant population size, (ii) exponential growth, and (iii) the flexible Bayesian skyline plot (BSP) model. The optimal coalescent model was also chosen using Bayes Factors. Note that in this study, the coalescent model is being used as a prior distribution for phylogenies, whose parameters are marginalised and ignored, and not as an explicit model of the population under study.

Genomic partition model

After the selection of the most appropriate molecular clock and coalescent models, each data set was split into 21 non-overlapping partitions 432 nt in length, beginning at the start codon of the *Core* gene. In order to estimate separate molecular clock parameters for each partition whilst simultaneously minimising estimation variance, we implemented a genomic partition model in BEAST v1.5.4 [21]. This model estimated separate molecular clock parameters and nucleotide frequencies for each partition, whilst all partitions share the same underlying nucleotide substitution model (as above), coalescent model parameters, and phylogenetic tree, thus making the most statistically efficient use of the available sequence information. XML files for performing these analyses are available on request. Partitions were kept of equal length (and not adjusted to coincide with gene boundaries) so that intra-genic variation could be measured and so that estimation uncertainty could be directly compared among genome regions. We deliberately ignored the alternate open reading frame in the *Core* gene, as its molecular evolution is under no selective constraints (e.g. [29]). This ORF therefore has no effect on the evolution of the HCV main reading frame

Partition specific dn/ds analyses

It was computationally-impractical to calculate *dn/ds* ratios for each partition whilst simultaneously incorporating phylogenetic uncertainty, hence we began by estimating a maximum likelihood (ML) tree for each of the three datasets using PhyML, under a HKY model of nucleotide substitution with gamma distributed site variation. The ratio of replacement-to-silent nucleotide substitution (*dn/ds*) and the transition/transversion ratio were calculated separately for each of the 21 non-

overlapping partitions defined above using PAML [30], given the ML tree and nucleotide alignment for each dataset.

Results

Model selection procedure

Table 1 shows the estimated statistical and evolutionary parameters for each model combination we investigated. For all three data sets, the relaxed clock model provided a much better fit than the strict clock model (BF>20). Although the choice of coalescent model did not significantly affect model fit (BF<3 for most comparisons), the MCMC under the constant size model failed to converge (data not shown). This is perhaps unsurprising, as phylogenies estimated from all data sets are star-like in shape (i.e. long terminal branches) and therefore poorly characterised by a constant-size coalescent model.

For all three data sets, the estimated genomic rate of evolution was consistent among all of the coalescent models investigated under the relaxed clock assumption (Table 1). For the among-host subtype 1a data set, the mean genome-wide rate was estimated to be 1.44 - 1.48 $\times 10^{-3}$ substitutions/site/year (among different coalescent models), while the equivalent rates for the subtype 1b data set were slightly lower (1.18 - 1.25 $\times 10^{-3}$ substitutions/site/year). The within-host genome-wide evolutionary rate was lower still than the two among-host datasets (1.11 - 1.13 $\times 10^{-3}$ substitutions/site/year). For all analyses, the lower confidence limit of the coefficient of variation statistic (which measures 'un-clock-likeness') was above zero, indicating statistically-significant variability in evolutionary rate among lineages. As expected for a continuous protein-coding region, the relative evolutionary rate of 1st and 2nd codon positions was significantly lower than that of the 3rd codon position (two-tailed T-test $p < 0.01$).

Genomic partition model

In light of the model selection results, the relaxed molecular clock was used in the genomic partition analysis. Since neither the BSP nor the exponential coalescent model was statistically favoured, we chose the model that exhibited the best MCMC mixing behaviour (BSP for the among-host datasets; exponential for the within-host dataset). For each genomic partition, we estimated the following parameters: (i) mean substitution rate, (ii) relaxed clock coefficient of variation, (iii) the relative rate of codon positions 1+2 to that of codon position 3. The estimated values for each of these parameters are shown in Figure 1, with both the point estimate (dots) and the 95% highest posterior density (HPD) confidence limits (vertical lines) shown for each parameter in each partition.

Figure 1a shows clear trends in evolutionary rate variation across the genome. In the majority of partitions the mean evolutionary rate of the among-host subtype 1a data set was slightly higher than that of subtype 1b (in agreement with the whole genome values presented in Table 1). For most of the non-structural genes (*p7, NS2, NS3, NS4a, NS5a* and *NS5b*), mean evolutionary rate was consistently about 1.0 $\times 10^{-3}$ substitutions/site/year, for all three datasets. However, notably higher

Table 1 Model Selection Analysis Results

Data set	Molecular clock model	Coalescent Model[a]	Marginal Log Likelihood	Genomic rate of evolution[b]($\times 10^{-3}$subs./site/year)	Relaxed clock coefficient of variation	Relative rate of evolution (codon positions 1 & 2)	Relative rate of evolution (codon position 3)
Among-host (1a)	Strict	Constant	-90901.35	1.30 (1.16 - 1.43)	*Not applicable*	0.72 (0.70 - 0.74)	1.56 (1.51 - 1.60)
	Relaxed	Constant	-90632.03	1.44 (1.00 - 1.84)	0.25 (0.21 - 0.30)	0.72 (0.70 - 0.74)	1.56 (1.51 - 1.60)
	Relaxed	Expo	-90632.39	1.47 (1.02 - 1.87)	0.24 (0.20 - 0.29)	0.72 (0.70 - 0.74)	1.56 (1.51 - 1.60)
	Relaxed	BSP	-90632.49	1.48 (1.09 - 1.84)	0.23 (0.20 - 0.27)	0.72 (0.70 - 0.75)	1.55 (1.51 - 1.60)
Among-host (1b)	Strict	Constant	-88288.70	1.04 (0.87 - 1.22)	*Not applicable*	0.66 (0.64 - 0.68)	1.68 (1.63 - 1.72)
	Relaxed	Constant	-88127.66	1.25 (0.73 - 1.73)	0.22 (0.18 - 0.26)	0.66 (0.64 - 0.68)	1.68 (1.64 - 1.72)
	Relaxed	Expo	-88125.80	1.24 (0.75 - 1.74)	0.21 (0.17 - 0.25)	0.66 (0.64 - 0.68)	1.68 (1.64 - 1.72)
	Relaxed	BSP	-88127.55	1.18 (0.67 - 1.65)	0.21 (0.17 - 0.25)	0.66 (0.64 - 0.68)	1.68 (1.63 - 1.72)
Within-host	Strict	Constant	-31070.20	1.12 (1.02 - 1.23)	*Not applicable*	0.58 (0.54 - 0.61)	1.85 (1.78 - 1.92)
	Relaxed	Constant	-31013.86	1.11 (0.97 - 1.23)	0.27 (0.19 - 0.37)	0.58 (0.54 - 0.61)	1.85 (1.78 - 1.92)
	Relaxed	Expo	-31013.56	1.13 (1.01 - 1.27)	0.30 (0.19 - 0.42)	0.58 (0.54 - 0.61)	1.85 (1.78 - 1.92)
	Relaxed	BSP	-31012.14	1.11 (0.98 - 1.24)	0.27 (0.19 - 0.34)	0.58 (0.54 - 0.61)	1.85 (1.78 - 1.92)

[a] Constant = constant population size, Expo = exponential growth, BSP = Bayesian skyline plot

[b] A single average rate of evolution estimated across the whole genome (no partitions)

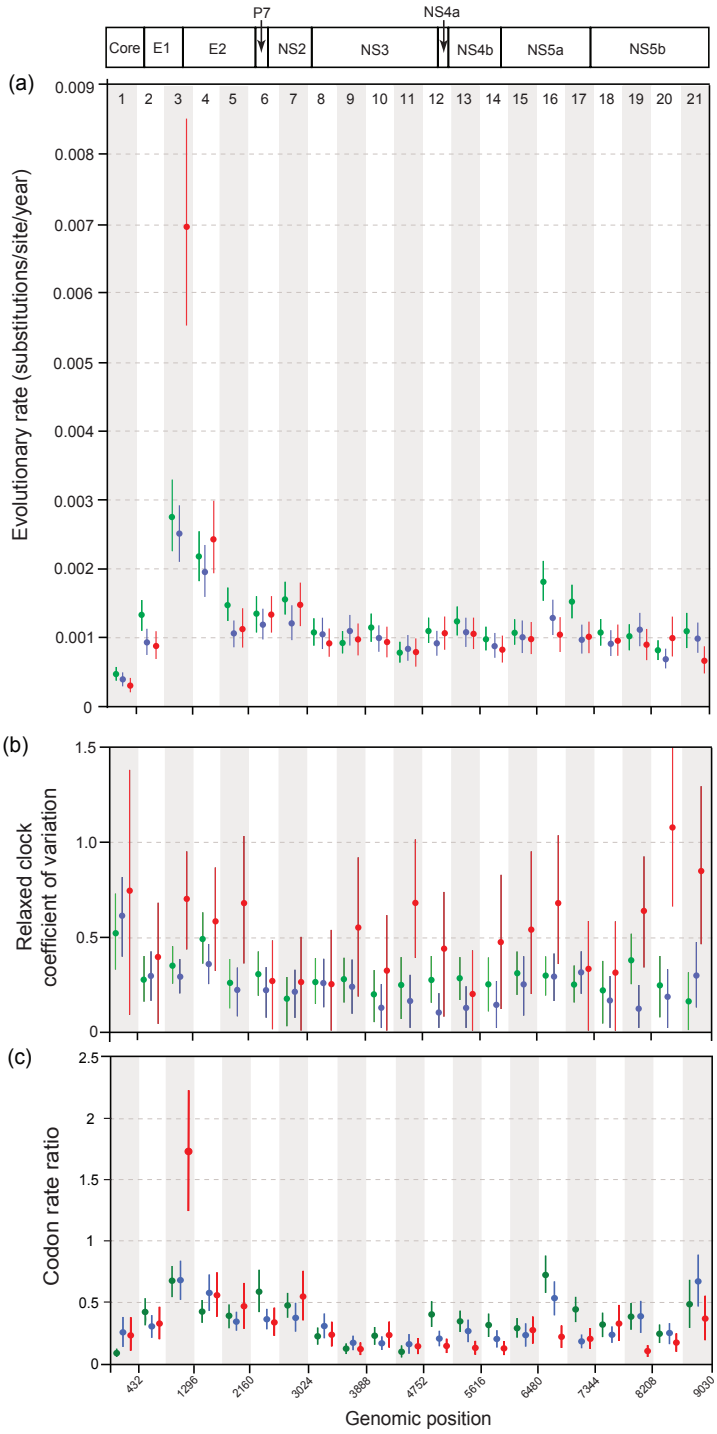

Figure 1 The molecular clock behaviour of the HCV genome. Three separate data sets are shown: among host subtype 1a (green), among host subtype 1b (blue) and within-host (red). Separate parameters were estimated for each of 21 partitions spanning the HCV coding region (see genome schematic and partition numbering at top of Figure). The alternating white and grey bars are for visual clarity only; nucleotide numbering according to the H77 reference genome is show at the bottom. (a) Estimated mean evolutionary rates. For each partition and data set, the vertical bar represents the range of the 95% HPD credible region and the circle represents the point estimate of the mean rate. (b) Estimated coefficient of variation (COV) parameters for each partition and data set, which represent the among-lineage rate heterogeneity. The vertical bars represent the range of the HPD credible region and the circle shows the estimated COV value. (c) Estimated codon rate ratio (CRR) values, which represent the ratio of the evolution rate at codon positions 1 and 2 to that at codon position 3. As before, the vertical bar represents the range of the 95% HPD credible region and the circle represents the point estimate of CRR.

rates were observed for the subtype 1a among-host data set, in the 16th and 17th partitions (3' end of the NS5a gene), which contain functionally important domains (see Discussion for details). Within the structural genes (*Core, E1* and *E2*) estimated mean evolutionary rates were low for the *Core* region (0.28 - 0.43 × 10^{-3} substitutions/site/year) and high in partitions 3 and 4 (the C-terminus of *E1* and N-terminus of *E2*). Partition 3 corresponds to the location of the hyper-variable region HVRI (2.5 - 6.9 × 10^{-3} substitutions/site/year). Partition 4, which includes the HVRII and III regions, also exhibited an elevated evolutionary rate in all three data sets (2.4 - 2.7 × 10^{-3} substitutions/site/year). Overall, variation in mean evolutionary rate is greater among genome regions than among the three data sets, with one very notable exception: the evolutionary rate of partition 3 (containing the HVRI) is remarkably higher for the within-host data set than for the two among-host data sets. The G/C content at each codon position was similar among datasets, being higher at the 3rd position than at the 1st or 2nd positions (Additional file 2, Figure S1), as previously reported [31].

For each partition, we also estimated the coefficient of variation (COV) statistic (Figure 1b). In general, the mean and variance of this parameter was significantly higher for the within-host dataset, hence among-branch rate variation is much higher in this data set than in the among-host data sets. In several partitions, the lower HPD confidence limit was close to zero, indicating that the strict clock hypothesis could not be excluded in these instances. Mean COV values for among-host data sets were typically around 0.2-0.3, in line with previous estimates for HIV [19] with the exception of the *Core* gene, which exhibited values >0.5. For the within-host dataset, COV estimates were also elevated for the last two genomic partitions (covering the C-terminus of *NS5b*).

We also estimated the ratio of the evolutionary rate at codon positions 1 & 2 to that at codon position 3 (the codon rate-ratio, CRR). This ratio can be computed concurrently with other molecular clock parameters and can be used to investigate selective pressures acting on gene sequences, because almost all changes at codon positions 1 & 2 are non-synonymous and the majority of changes at codon position 3 are synonymous. Estimates of the CRR for each genomic partition are shown in Figure 1c. In general, the CRR was low between partitions 8 and 20, corresponding to most of the non-structural genome region, indicating on average strong selective constraint. Partitions 16 and 21, however, have raised CRR values for the among-host data sets. CRR values are slightly higher in the *E1*, *E2* and *NS2* genes, with a particularly high ratio observed for the within-host data set in partition 3.

To determine whether the elevated evolutionary rate and correspondingly high CRR of partition 3 in the within-host data set was independent of the 3rd codon position rate, we plotted the absolute rates for the 1st +2nd versus 3rd codon positions for each partition (Additional file 3, Figure S2). As expected, the 1st+2nd position rate was much lower than the 3rd position rate for all partitions in the among-host datasets. For partition 3 of intra-host dataset, the 1st+2nd position rate (0.008 subs./site/year) was greater than the 3rd position rate (0.005 subs./site/year). However, in this partition the 3rd position rates for the intra-host datasets were also significantly elevated. The lowest 3rd position rates were observed in partitions 1 and 21. This is consistent with the presence of RNA secondary structure (stem-loops) in these regions of the HCV coding region [32]. This structure will likely impose selective constraints on 3rd codon positions, resulting in a lower evolutionary rate at silent sites. However, we observed no consistent effect of RNA secondary structure on CRR values: in partition 21 the CRR is raised, which could reflect a lower rate of silent change, whereas the CRR in partition 1 is very low. When evolutionary rates vary among silent sites, *dn/ds* ratios are commonly interpreted as measures of the *difference* in selection pressure between replacement and silent sites [33] and we propose that the CRR ratio should be interpreted similarly.

Visual inspection of Figure 1 suggests that genomic partitions with high evolutionary rates also have a high CRR. To test for correlations among the three molecular clock parameters (mean rate, COV, and CRR), Figure 2 shows scatterplots among all estimated parameter values. There is a clear positive correlation between mean rate and CRR (Figure 2a; $p < 0.001$) which is robust to the exclusion of the outlying data point ($p < 0.001$). In contrast, there is no clear correlation between mean rate and COV (Figure 2b; $p = 0.34$), nor between CRR and COV (Figure 2c; $p = 0.67$). Figures 2b and 2c do, however, clearly illustrate the higher COV values for the within-host data set.

Lastly, to investigate the relationship between CRR and the more widely-used *dn/ds* ratio, we estimated *dn/ds* values for each partition and data set using PAML [30] (see Methods). Figure 3 shows the scatterplot of *dn/ds* versus CRR values, which, as expected, are strongly correlated ($p < 0.001$). The estimated regression relationship between these two variables is *dn/ds* = 2.44. CRR (assuming no error distribution for the *dn/ds* values; also robust to the exclusion of the outlying data point; $p < 0.001$).

Discussion

Since its discovery in 1989, the molecular evolution of HCV has been investigated using a wide variety of

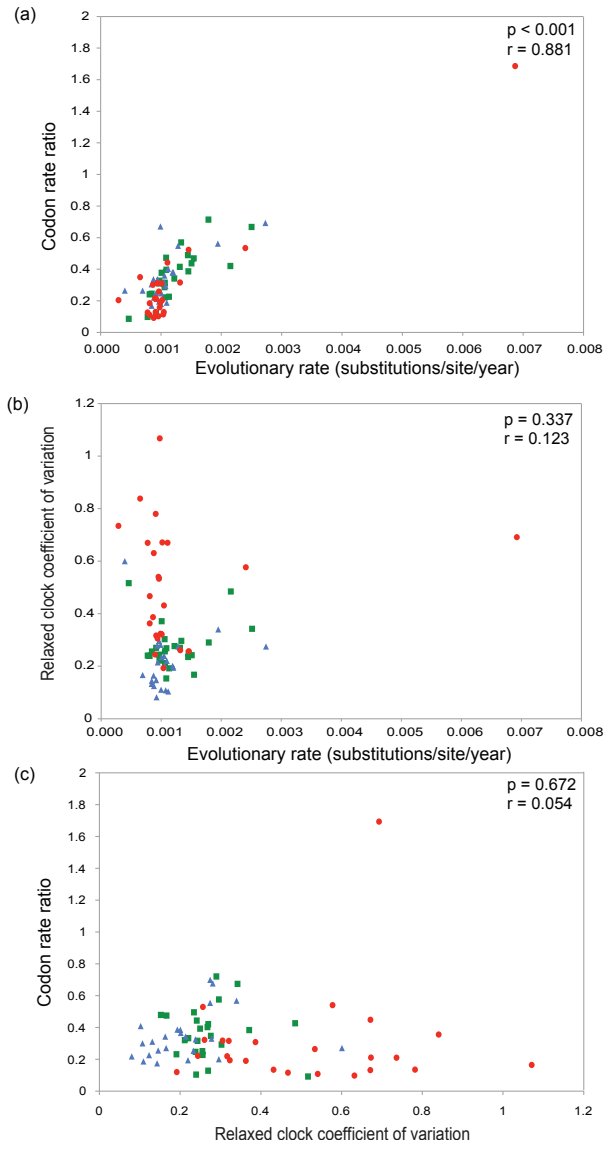

Figure 2 Scatterplots of the three molecular clock parameter estimates obtained for each partition, calculated using the uncorrelated lognormal (UCLN) relaxed clock model. Colouring is the same as that in Figure 1: among host subtype 1a data set (green squares), among host subtype 1b data set (blue triangles) and within-host data set (red circles). (a) Plot of mean evolutionary rate versus the coefficient of variation. (b) Plot of mean evolutionary rate versus the codon rate ration. (c) Plot of the coefficient of variation versus the codon rate ration. See main text for full description of each parameter. For each plot, the correlation coefficient (r) and statistical significance (p) of the relationships are given.

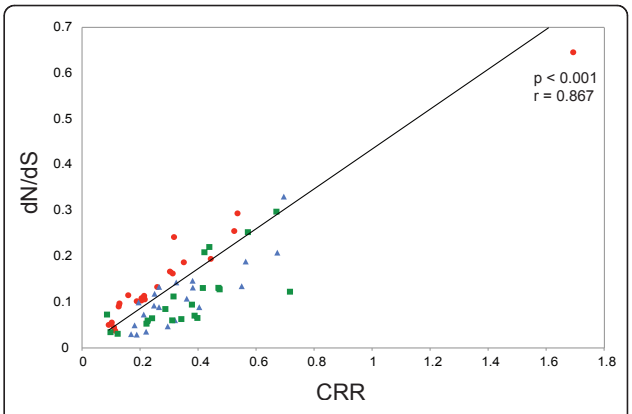

Figure 3 Scatterplot of the codon rate ratio estimate for each partition, versus the average dn/ds ratio, calculated using PAML. Colouring is the same as that in Figure 1: among host subtype 1a data set (green squares), among host subtype 1b data set (blue triangles) and within-host data set (red circles).

approaches. Early studies approximated HCV evolutionary rates by simply counting the number of observed changes between sequences sampled at different times from infected patients [34,35] or from a chimpanzee [36]. Subsequent studies used nucleotide substitution models to estimate genetic distances, but commonly focused only on sub-genomic regions, particularly the *Core*, *E1/E2* and *NS5B* genes (e.g. [14,37]). Rates of evolution have been estimated using (i) relative-rate methods (e.g. Ina *et al* [38]), (ii) linear regressions of genetic distances against sampling times (e.g. Tanaka *et al.* [39]), (iii) maximum likelihood phylogenetic methods (e.g.[15]) and (iv) Bayesian phylogenetic methods (e.g. [40]). Some analyses were performed on among-host data, some on within-host sequences, and others on a combination of both. Unsurprisingly, estimates of the tempo of HCV evolution from these various studies have been highly variable and are impossible to compare directly due to the different methodologies and genome regions employed.

Our study of HCV molecular evolution has employed powerful statistical methods [20] in a consistent manner, enabling us to make reliable inferences about how HCV sequence evolution varies among genome regions, and how it varies between different levels of organisation. As expected, the variation we observed in evolutionary rate across the genome closely matches genomic variation in overall HCV genetic diversity (previously measured in [11,41]). While most of the HCV genome evolves at ~0.001 substitutions/site/year, a rate very typical of RNA viruses [42], the E1/E2 region (partitions 3 and 4) exhibited the highest evolutionary rates, consistent with previous reports (e.g. Itakura *et al.* [23]). This region contains several known antibody epitopes and hypervariable regions, and our high CRR and *dn/ds* values in these regions confirm the action of positive selection [5,8,23].

A striking result from this study was the elevated evolutionary rate in the intra-host dataset for partition 3 when compared to the among-host dataset. Several explanations are possible. First, we might hypothesise

that saturation of nucleotide changes (and hence underestimation of genetic distance) is occurring at the among-host level but not at the within-host level. Although this phenomenon is certainly important for rapidly-evolving viruses when evolution measured over several decades is extrapolated to thousands of years (e.g. [43]), it is very unlikely to be responsible for our result, since our within-host and among-host timescales differ only by a factor of 3. Additionally, we found no evidence of saturation at the 3rd codon position in partitions 3 and 4 for the within-host dataset (data not shown). A second explanation follows from the primary difference between the within- and among-host datasets: the latter contains transmission events while the former does not. Upon transmission to a new host, specific mutations that conferred a fitness advantage in the immune environment of the donor may be lost or quickly revert to wild-type in the new environment of the recipient. This phenomenon has been reported for both HCV [44-47] and HIV [48] and is consistent with the observation of an elevated rate in the epitope-rich region (*E1/E2*) of the HCV genome when transmission bottlenecks are absent (i.e. the within-host dataset). Reversion is also consistent with the elevated CRR in this region, which indicates a higher net rate of adaptation within hosts. A third and intriguing possibility is that slowly-evolving lineages within a host are preferentially-transmitted, resulting in a lower long-term evolutionary rate [1]. This is consistent with the high among-branch rate variation (COV) observed within-hosts here, and for HIV-1 elsewhere [19], suggesting that there is significant variation in the rate of evolution of different lineages within an infected host. However, preferential transmission of slower-evolving lineages should result in a lower among-host long-term replication rate (and thus a lower 3rd codon position rate) equally across all partitions - which is not observed in our data (Additional file 3, Figure S2).

We did observe a consistently higher genome-wide among-host evolutionary rate for subtype 1a in comparison with subtype 1b. This difference could be a consequence of the major modes of transmission of that characterise each subtype: subtype 1a is more commonly associated with intravenous drug use and subtype 1b with past blood transfusions. If within-host HCV evolution is faster at the start of chronic infection (possibly due to adaptation to the new host; [41]) then the long-term among-host rate of evolution will depend to some extent on the rate of transmission [24]. A similar phenomenon, albeit more extreme, has been previously reported for HTLV-II, for which differences in the rate of transmission among different risk groups greatly affect the long-term evolutionary rate [49]. Our data cannot indicate whether average evolutionary rates vary during the course of a single chronic infection, and this question remains an important area for future research.

A higher rate evolution for subtype 1a was especially pronounced for partitions 16 and 17, which contain functionally important genome regions within the NS5a gene. Interestingly, this elevated rate resulted from an increase in 1+2nd substitutions, suggesting the presence of selected sites for this subtype. NS5a forms a necessary part of the replication complex but its function is not fully understood [50]. It is involved in cellular pathways including the interferon response [51] and genetic variation within NS5a has been associated with response to anti-viral drug therapy. Specifically, partition 16 contains the interferon sensitivity-determining region (ISDR), variation within which is reported to predict response to interferon drug therapy [52], although inconsistently between subtypes 1a and 1b [53] and with different results observed in Japanese and European cohorts [50]. The PKR binding domain (which includes the ISDR) and the "V3" region, are also included in partition 16, changes within which may be related to treatment outcome [54]. Similarly, partition 17 contains the less well-studied interferon/ribavirin-resistance determining region (IRRDR) [55], in which excess mutations in patients infected with subtype 1b were more likely to respond to therapy [56]. The possible difference in selective pressure between 1a and 1b that we observed in this region is consistent with subtype-specific differences in resistance mutations in NS5a against the potent viral inhibitor BMS-790052 [57]. Information on drug treatment was unavailable for the subjects included in this study, and although differences in treatments are unlikely to account for the observed differences in this region, the possibility cannot be excluded.

Conclusions

Because our study employed powerful statistical methods on whole genome sequences, we have been able to quantify the variation in HCV evolutionary dynamics at different scales of organisation for the first time, and thereby confirm that scale-dependent differences in rate are not restricted to HIV and may represent a common feature of chronic RNA viral infection. We posit that the most likely explanation of our current data is that host-specific reversion events are responsible for an elevated rate of evolution and adaptation in the *E1/E2* region within-hosts compared to among-hosts.

Additional material

Additional file 1: Table S1: Accession numbers and dates of sampling. Accession numbers and isolate sampling dates of all sequences used in this study.

Additional file 2: Figure S1: The G/C content at each codon position for three datasets. Three separate data sets are shown: among host subtype 1a (green), among host subtype 1b (blue) and within-host (red). Separate parameters were estimated for each of 21 partitions spanning the HCV coding region (see genome schematic and partition numbering at top of Figure). The alternating white and grey bars are for visual clarity only.

Additional file 3: Figure S2: Absolute rates for the 1st+2nd versus 3rd codon positions for each partition. Three separate data sets are shown: among host subtype 1a (green), among host subtype 1b (blue) and within-host (red). Squares represent the rate of the 1st+2nd positions, circles the 3rd position. The symbols are offset within each partition for visual clarity only. Separate parameters were estimated for each of 21 partitions spanning the HCV coding region (see genome schematic and partition numbering at top of Figure).

Acknowledgements
JP thanks Nicole Zitzmann, Ellie Barnes, Vicki Flemming and Isla Humphreys for discussions. RRG was supported by the T-32 NIH Training Grant in Cancer Biology, JP by the NERC (UK), OGP & AK by the Royal Society, and PL by the Fund for Scientific Research (FWO) Flanders.

Author details
[1]Department of Pathology, Immunology and Laboratory Medicine, University of Florida, Gainesville, FL, USA. [2]Emerging Pathogens Institute, University of Florida, Gainesville, FL, USA. [3]Kitson Consulting, Bristol, BS8 3UL, UK. [4]Department of Microbiology and Immunology, Katholieke Universiteit Leuven, Leuven, Belgium. [5]Department of Zoology, Oxford University, South Parks Road, Oxford, OX1 3PS, UK.

Authors' contributions
OGP conceived the project. RRG and JP implemented analyses. RRG, JP and OGP interpreted data and wrote the manuscript. PL, AK, and MS provided assistance in running the analyses and interpreting data. All authors read and approved the manuscript.

Received: 28 February 2011 Accepted: 19 May 2011
Published: 19 May 2011

References
1. Pybus OG, Rambaut A: **Evolutionary analysis of the dynamics of viral infectious disease.** *Nature Reviews Genetics* 2009, **10**:540-550.
2. Grenfell BT, Pybus OG, Gog JR, Wood JL, Daly JM, Mumford JA, Holmes EC: **Unifying the epidemiological and evolutionary dynamics of pathogens.** *Science* 2004, **303**:327-332.
3. Levrero M: **Viral hepatitis and liver cancer: the case of hepatitis C.** *Oncogene* 2006, **25**:3834-3847.
4. **Hepatitis-C FAQs for the Public.** [http://www.cdc.gov/hepatitis/C/cFAQ.htm#statistics].
5. Farci P, Shimoda A, Coiana A, Diaz G, Peddis G, Melpolder JC, Strazzera A, Chien DY, Munoz SJ, Balestrieri A, Purcell RH, Alter HJ: **The outcome of acute hepatitis C predicted by the evolution of the viral quasispecies.** *Science* 2000, **288**:339-344.
6. Ray SC, Wang YM, Laeyendecker O, Ticehurst JR, Villano SA, Thomas DL: **Acute hepatitis C virus structural gene sequences as predictors of persistent viremia: hypervariable region 1 as a decoy.** *Journal of Virology* 1999, **73**:2938-2946.
7. Abbate I, Lo Iacono O, Di Stefano R, Cappiello G, Girardi E, Longo R, Ferraro D, Antonucci G, Di Marco V, Solmone M, Craxì A, Ippolito G, Capobianchi MR: **HVR-1 quasispecies modifications occur early and are correlated to initial but not sustained response in HCV-infected patients treated with pegylated- or standard-interferon and ribavirin.** *Journal of Hepatology* 2004, **40**:831-836.
8. Sheridan I, Pybus OG, Holmes EC, Klenerman P: **High-resolution phylogenetic analysis of hepatitis C virus adaptation and its relationship to disease progression.** *Journal of Virology* 2004, **78**:3447-3454.
9. Arenas JI, Gallegos-Orozco JF, Laskus T, Wilkinson J, Khatib A, Fasola C, Adair D, Radkowski M, Kibler KV, Nowicki M, Douglas D, Williams J, Netto G, Mulligan D, Klintmalm G, Rakela J, Vargas HE: **Hepatitis C virus quasi-species dynamics predict progression of fibrosis after liver transplantation.** *The Journal of Infectious Diseases* 2004, **189**:2037-2046.
10. Booth JC, Kumar U, Webster D, Monjardino J, Thomas HC: **Comparison of the rate of sequence variation in the hypervariable region of E2/NS1 region of hepatitis C virus in normal and hypogammaglobulinemic patients.** *Hepatology* 1998, **27**:223-227.
11. Salemi M, Vandamme A: **Hepatitis C virus evolutionary patterns studied through analysis of full-genome sequences.** *Journal of Molecular Evolution* 2002, **54**:62-70.
12. Moradpour D, Penin F, Rice C: **Replication of hepatitis C virus.** *Nature Reviews Microbiology* 2007, **5**:453-463.
13. Bartosch B, Verney G, Dreux M, Donot P, Morice Y, Penin F, Pawlotsky J, Lavillette D, Cosset F: **An interplay between hypervariable region 1 of the hepatitis C virus E2 glycoprotein, the scavenger receptor BI, and high-density lipoprotein promotes both enhancement of infection and protection against neutralizing antibodies.** *Journal of Virology* 2005, **79**:8217-8229.
14. Allain J, Dong Y, Vandamme A, Moulton V, Salemi M: **Evolutionary rate and genetic drift of hepatitis C virus are not correlated with the host immune response: studies of infected donor-recipient clusters.** *Journal of Virology* 2000, **74**:2541-2549.
15. Pybus OG, Charleston M, Gupta S, Rambaut A, Holmes E, Harvey P: **The epidemic behavior of the hepatitis C virus.** *Science* 2001, **292**:2323-2325.
16. Pybus OG, Barnes E, Taggart R, Lemey P, Markov P, Rasachak B, Syhavong B, Phetsouvanah R, Sheridan I, Humphreys I, Lu L, Newton PN, Klenerman P: **Genetic history of hepatitis C virus in East Asia.** *Journal of Virology* 2009, **83**:1071-1082.
17. Drummond AJ, Pybus OG, Rambaut A, Forsberg R, Rodrigo AG: **Measurably evolving populations.** *Trends in Ecology and Evolution* 2003, **18**:481-488.
18. Lemey P, Salemi M, Wang B, Duffy M, Hall WH, Saksena NK, Vandamme AM: **Site stripping based on likelihood ratio reduction is a useful tool to evaluate the impact of non-clock-like behavior on viral phylogenetic reconstructions.** *FEMS Immunol Med Microbiol* 2003, **39**:125-132.
19. Lemey P, Rambaut A, Pybus OG: **HIV evolutionary dynamics within and among hosts.** *AIDS Reviews* 2006, **8**:125-140.
20. Drummond A, Ho S, Phillips M, Rambaut A: **Relaxed phylogenetics and dating with confidence.** *PLoS Biology* 2006, **4**:e88.
21. Drummond AJ, Rambaut A: **BEAST: Bayesian evolutionary analysis by sampling trees.** *BMC Evolutionary Biology* 2007, **7**:214.
22. Power J, Davidson F, O'Riordan J, Simmonds P, Yap P, Lawlor E: **Hepatitis C infection from anti-D immunoglobulin.** *Lancet* 1995, **346**:372-373.
23. Itakura J, Nagayama K, Enomoto N, Hamano K, Sakamoto N, Fanning L, Kenny-Walsh E, Shanahan F, Watanabe M: **Viral load change and sequential evolution of entire hepatitis C virus genome in Irish recipients of single source-contaminated anti-D immunoglobulin*.** *Journal of Viral Hepatitis* 2005, **12**:594-603.
24. McAllister J, Casino C, Davidson F, Power J, Lawlor E, Yap P, Simmonds P, Smith D: **Long-term evolution of the hypervariable region of hepatitis C virus in a common-source-infected cohort.** *Journal of Virology* 1998, **72**:4893-4905.
25. Kass R, Raftey A: **Bayes Factors.** *Journal of the American Statistical Association* 1995, **90**:773-795.
26. Suchard M, Weiss R, Sincheimer J: **Bayesian selection of continuous-time Markov chain evolutionary models.** *Molecular Biology & Evolution* 2001, **18**:1001-1013.
27. Suchard MA, Weiss RE, Sincheimer JS: **Bayesian selection of continuous-time Markov chain evolutionary models.** *Molecular Biology & Evolution* 2001, **18**:1001-1013.
28. Shapiro B, Rambaut A, Drummond AJ: **Choosing appropriate substitution models for the phylogenetic analysis of protein-coding sequences.** *Molecular Biology & Evolution* 2006, **23**:7-9.
29. Cristina J, Lopez F, Moratorio G, López L, Vasquez S, García-Aguirre L, Chunga A: **Hepatitis C virus F protein sequence reveals a lack of functional constraints and a variable pattern of amino acid substitution.** *Journal of General Virology* 2005, **86**:115-120.
30. Yang Z: **PAML 4: phylogenetic analysis by maximum likelihood.** *Molecular Biology & Evolution* 2007, **24**:1586-1591.
31. Smith DB, Simmonds P: **Characteristics of nucleotide substitution in the hepatitis C virus genome: constraints on sequence change in coding**

regions at both ends of the genome. *Journal of Molecular Evolution* 1997, **45**:238-246.
32. Tuplin A, Wood J, Evans DJ, Patel AH, Simmonds P: **Thermodynamic and phylogenetic prediction of RNA secondary structures in the coding region of hepatitis C virus.** *RNA* 2002, **8**:824-841.
33. Pybus OG, Shapiro B: **Natural selection and adaptation of molecular sequences.** In *The Phylogenetic Handbook*. Edited by: Lemey P, Salemi M, Vandamme A. Cambridge: Cambridge University Press; 2009:406-418.
34. Ogata N, Alter H, Miller R, Purcell R: **Nucleotide sequence and mutation rate of the H strain of hepatitis C virus.** *Proc Natl Acad Sci USA* 1991, **88**:3392-3396.
35. Abe K, Inchauspe G, Fujisawa K: **Genomic characterization and mutation rate of hepatitis C virus isolated from a patient who contracted hepatitis during an epidemic of non-A, non-B hepatitis in Japan.** *Journal of General Virology* 1992, **73**:2725-2729.
36. Okamoto H, Kojima M, Okada S, Yoshizawa H, Iizuka H, Tanaka T, Muchmore E, Peterson D, Ito Y, Mishiro S: **Genetic drift of hepatitis C virus during an 8.2-year infection in a chimpanzee: variability and stability.** *Virology* 1992, **190**:894-899.
37. Cantaloube J, Biagini P, Attoui H, Gallian P, de Micco P, de Lamballerie X: **Evolution of hepatitis C virus in blood donors and their respective recipients.** *Journal of General Virology* 2003, **84**:441-446.
38. Ina Y, Mizokami M, Ohba K, Gojobori T: **Reduction of synonymous substitutions in the core protein gene of hepatitis C virus.** *Journal of Molecular Evolution* 1994, **38**:50-56.
39. Tanaka Y, Hanada K, Mizokami M, Yeo A, Shih J, Gojobori T, Alter H: **Inaugural Article: A comparison of the molecular clock of hepatitis C virus in the United States and Japan predicts that hepatocellular carcinoma incidence in the United States will increase over the next two decades.** *Proc Natl Acad Sci USA* 2002, **99**:15584-15589.
40. Magiorkinis G, Magiorkinis E, Paraskevis D, Ho S, Shapiro B, Pybus OG, Allain J, Hatzakis A: **The global spread of hepatitis C virus 1a and 1b: a phylodynamic and phylogeographic analysis.** *PLoS Medicine* 2009, **6**: e1000198.
41. Simmonds P, Balfe P, Peutherer JF, Ludlam CA, Bishop JO, Brown AJ: **Human immunodeficiency virus-infected individuals contain provirus in small numbers of peripheral mononuclear cells and at low copy numbers.** *Journal of Virology* 1990, **64**:864-872.
42. Jenkins G, Rambaut A, Pybus O, Holmes E: **Rates of molecular evolution in RNA viruses: a quantitative phylogenetic analysis.** *Journal of Molecular Evolution* 2002, **54**:156-165.
43. Worobey M, Telfer P, Souquière S, Hunter M, Coleman CA, Metzger MJ, Reed P, Makuwa M, Hearn G, Honarvar S, Roques P, Apetrei C, Kazanji M, Marx PA: **Island biogeography reveals the deep history of SIV.** *Science* 2010, **329**:1487.
44. Ray SC, Fanning L, Wang XH, Netski DM, Kenny-Walsh E, Thomas DL: **Divergent and convergent evolution after a common-source outbreak of hepatitis C virus.** *Journal of Experimental Medicine* 2005, **201**:1753-1759.
45. Cox AL, Mosbruger T, Mao Q, Liu Z, Wang XH, Yang HC, Sidney J, Sette A, Pardoll D, Thomas DL, Ray SC: **Cellular immune selection with hepatitis C virus persistence in humans.** *Journal of Experimental Medicine* 2005, **201**:1741-1752.
46. Tester I, Smyk-Pearson S, Wang P, Wertheimer A, Yao E, Lewinsohn DM, Tavis JE, Rosen HR: **Immune evasion versus recovery after acute hepatitis C virus infection from a shared source.** *Journal of Experimental Medicine* 2005, **201**:1725-1731.
47. Timm J, Lauer GM, Kavanagh DG, Sheridan I, Kim AY, Lucas M, Pillay T, Ouchi K, Reyor LL, Schulze zur Wiesch J, Gandhi RT, Chung RT, Bhardwaj N, Klenerman P, Walker BD, Allen TM: **CD8 epitope escape and reversion in acute HCV infection.** *Journal of Experimental Medicine* 2004, **200**:1593-1604.
48. Herbeck JT, Nickle DC, Learn GH, Gottlieb GS, Curlin ME, Heath L, Mullins JI: **Human immunodeficiency virus type 1 env evolves toward ancestral states upon transmission to a new host.** *Journal of Virology* 2006, **80**:1637-1644.
49. Salemi M, Lewis M, Egan JF, Hall WW, Desmyter J, Vandamme AM: **Different population dynamics of human T cell lymphotropic virus type II in intravenous drug users compared with endemically infected tribes.** *Proc Natl Acad Sci USA* 1999, **96**:13253-13258.
50. Pawlotsky JM: **Hepatitis C virus (HCV) NS5A protein: role in HCV replication and resistance to interferon-alpha.** *Journal of Viral Hepatitis* 1999, **6(Suppl 1)**:47-48.
51. Song J, Fujii M, Wang F, Itoh M, Hotta H: **The NS5A protein of hepatitis C virus partially inhibits the antiviral activity of interferon.** *Journal of General Virology* 1999, **80**:879-886.
52. Enomoto N, Sakuma I, Asahina Y, Kurosaki M, Murakami T, Yamamoto C, Izumi N, Marumo F, Sato C: **Comparison of full-length sequences of interferon-sensitive and resistant hepatitis C virus 1b. Sensitivity to interferon is conferred by amino acid substitutions in the NS5A region.** *Journal of Clinical Investigations* 1995, **96**:224-230.
53. Torres-Puente M, Cuevas JM, Jiménez-Hernández N, Bracho MA, García-Robles I, Carnicer F, del Olmo J, Ortega E, Moya A, González-Candelas F: **Hepatitis C virus and the controversial role of the interferon sensitivity determining region in the response to interferon treatment.** *Journal of Medical Virology* 2008, **80**:247-253.
54. Nousbaum J, Polyak SJ, Ray SC, Sullivan DG, Larson AM, Carithers RL, Gretch DR: **Prospective characterization of full-length hepatitis C virus NS5A quasispecies during induction and combination antiviral therapy.** *Journal of Virology* 2000, **74**:9028-9038.
55. El-Shamy A, Nagano-Fujii M, Sasase N, Imoto S, Kim SR, Hotta H: **Sequence variation in hepatitis C virus nonstructural protein 5A predicts clinical outcome of pegylated interferon/ribavirin combination therapy.** *Hepatology* 2008, **48**:38-47.
56. El-Shamy A, Kim SR, Ide YH, Sasase N, Imoto S, Deng L, Shoji I, Hotta H: **Polymorphisms of Hepatitis C Virus Non-Structural Protein 5A and Core Protein and Clinical Outcome of Pegylated-Interferon/Ribavirin Combination Therapy.** *Intervirology* 2011.
57. Fridell RA, Qiu D, Wang C, Valera L, Gao M: **Resistance analysis of the hepatitis C virus NS5A inhibitor BMS-790052 in an in vitro replicon system.** *Antimicrob Agents Chemother* 2010, **54**:3641-3650.

doi:10.1186/1471-2148-11-131
Cite this article as: Gray *et al.*: The mode and tempo of hepatitis C virus evolution within and among hosts. *BMC Evolutionary Biology* 2011 **11**:131.